Magnetization dynamics under a quasiperiodic magnetic field

David Laroze[1,2], David Becerra-Alonso[3], Jason. A. C. Gallas[4], and Harald Pleiner[1]

[1]Max Planck Institute for Polymer Research, 55021 Mainz, Germany
[2]Instituto de Alta Investigación, Universidad de Tarapacá, Casilla 7D, Arica, Chile
[3]ETEA, Universidad Loyola Andalucía, C/ Escritor Castilla Aguayo 4, Cordoba, Spain
[4]Instituto de Física, Universidade Federal do Rio Grande do Sul, 91501-970 Porto Alegre, Brazil

In the present work we study the deterministic spin dynamics of an anisotropic magnetic particle in the presence of a time dependent magnetic field using the Landau-Lifshitz-Gilbert equation. In particular, we study the case when the magnetic field consists in two terms. One is perpendicular to the anisotropy direction and has quasiperiodic time dependence, while the other term is constant and parallel to the anisotropy direction. We numerically characterize the dynamical behavior of the system by monitoring the Lyapunov exponents, and by calculating Poincaré sections and Fourier spectra. In addition, we calculate analytically the corresponding Melnikov function which gives us the bifurcations of the homoclinic orbits. We find a rather complicated landscape of sometimes closely intermingled chaotic and non-chaotic areas in parameters space. Finally, we show that the system exhibits strange nonchaotic attractors.

Index Terms— **Chaotic dynamics, Lyapunov spectrum, magnetization dynamics, Quasiperiodic modulation.**

I. INTRODUCTION

NONLINEAR problems have been widely studied in magnetism, cf. Refs. [1–2]. Models have been used in both, discrete [3–8] and continuous magnetic systems [9]. Recently, the chaotic behavior of an anisotropic particle under a periodic magnetic field was extensively studied in Refs. [7–8]. Several experiments of chaotic behaviors in magnetic systems have been reported [10–13]. Typical magnetic samples are yttrium iron garnet spheres [10]. It is worth mentioning that different types of routes to chaos have been found using ferromagnetic resonance techniques, such as period-doubling cascades, quasi-periodic routes to chaos, or intermittent routes to chaos. This implies that there is no universal mechanism leading to chaos in these systems, and therefore a theoretical description turns out to be highly complicated.

On the other hand, quasiperiodically forced systems have been theoretically and experientially studied in different branches of physics over the last decades [14–17]. This type of forcing is the natural extension of the single frequency forcing, and indeed one can expect a more complex behavior. In fact, the simplest invariant sets are tori-shaped ones [15]. Moreover, there are commonly other types of attractors, called *strange nonchaotic attractors*, where "strange" implies a complicated and non-smooth attractor topology, and "nonchaotic" indicates that it does not have sensitive dependence on the initial conditions [17].

The aim of this paper is to investigate the dynamical behavior of an anisotropic magnetic particle under the influence of both, a constant and a time dependent external magnetic field. The latter is assumed to have a two-frequency quasiperiodic (QP) modulation perpendicular to the anisotropy direction, while the constant field is parallel to the anisotropy axis. We calculate numerically the Lyapunov exponents, the Poincaré section, and the Fourier spectrum, thus characterizing the dynamical behavior. In particular, the maximum Lyapunov exponent is presented in the form of two-dimensional maps as a function of the relevant parameters of the system [18]. In addition, in order to make a theoretical complement to our numerical simulations, we calculate analytically the Melnikov function [2], which is a tool to determine chaotic regimes when chaos arises as an instability of an homoclinic orbit (HO).

II. MODEL

We consider the dynamics of the magnetization $\mathbf{M}$ of a monodomain magnetic particle. The temporal evolution of the system can be modeled by the dimensionless LLG equation:

$$\frac{d\mathbf{m}}{d\tau} = -\mathbf{m} \times \mathbf{\Gamma} - \eta \mathbf{m} \times (\mathbf{m} \times \mathbf{\Gamma}), \qquad (1)$$

where $\mathbf{m} = \mathbf{M}/M_s$ and $\tau = t|\gamma|M_s/\kappa$ with $\kappa = 1 + \eta^2$. Here M_s is the saturation magnetization that leads to $|\mathbf{m}| = 1$, and γ is the gyromagnetic factor, which is associated with the electron spin and whose numerical value is approximately given by $|\gamma| = |\gamma_e| \mu_0 \approx 2.21 \times 10^5 \, m A^{-1} s^{-1}$. Also, η denotes the dimensionless phenomenological damping coefficient which is a material property with typical values of order 10^{-4} to 10^{-3} in garnets and 10^{-2} or larger in cobalt or in nickel or in permalloy [7], which produces $1/\kappa \approx 0.99 \approx 1$. Typical experimental values of M_s are, e.g. $M_{s[Co]} \approx 1.42 \times 10^6 \, A/m \approx 17.8 \, kOe$ for cobalt materials and $M_{s[Ni]} \approx 4.8 \times 10^5 \, A/m \approx 6 \, kOe$ for nickel materials, leading to $|\gamma|M_{s[Co]} \approx 308 \, GHz$ and $|\gamma|M_{s[Ni]} \approx 106 \, GHz$, respectively. This implies that $(|\gamma|M_s)^{-1} \approx 3 \, ps$ and $(|\gamma|M_s)^{-1} \approx 6 \, ps$, respectively. Also, let us mention that in these materials the macrospin approximation (monodomain particles) is valid for particles with sizes of $10-20 \, nm$, because for smaller sizes surface anisotropy effects are relevant [19] and for larger sizes non-uniform magnetic states appear, like vortices in cobalt

nanodots. In addition, the shape of the nanoparticle plays an important role in the macrospin approximation [20].

The effective magnetic field, $\mathbf{\Gamma}$, acting on the magnetization is given by $\mathbf{\Gamma} = \mathbf{h} + \beta(\mathbf{m}\cdot\hat{\mathbf{n}})\hat{\mathbf{n}}$, where $\mathbf{h}$ is the external magnetic field and β measures the anisotropy along the $\hat{\mathbf{n}}$ axis, which we take as the z-axis in the following. This anisotropy is uniaxial and the constant β depends on the specific substance and sample shape, and can be positive or negative. The external magnetic field $\mathbf{h}$ comprises both, a constant and a time dependent modulation [14], that means

$$\mathbf{h} = h_z\hat{\mathbf{z}} + h_x(\tau)\hat{\mathbf{x}} = h_z\hat{\mathbf{z}} + \left(h_{x1}\sin(\Omega_1\tau) + h_{x2}\sin(\Omega_2\tau)\right)\hat{\mathbf{x}}, \quad (2)$$

where the coefficients $\{h_z, h_{x1}, \Omega_1, h_{x2}, \Omega_2\}$ are constants. Within on this dimensional scaling, the dimensionless fields and frequencies are $\mathbf{h} = \mathbf{H}/M_s$ and $\Omega_j = \omega_j\kappa/(\gamma M_s)$ with $j = (1,2)$. Since the amplitude of field $\mathbf{H}$ and the frequencies are measured in units of M_s and (γM_s), respectively, one finds that for cobalt or nickel material the typical order of magnitude is $10^0 - 10^1\ kOe$ and GHz. Here, we vary theses values in the same range of magnitude. Notice, that there are two relevant cases for the ratio of the frequencies Ω_1/Ω_2. When Ω_1/Ω_2 is rational, the system is periodically forced, whereas an irrational Ω_1/Ω_2 produces a two-frequency QP forcing.

For zero damping $(\eta = 0)$ and without parametric forcing $(h_{x1} = h_{x2} = 0)$ Eq. (1) is conservative, and it can be derived from a free energy, $d\mathbf{m}/d\tau = \mathbf{m}\times\nabla_{\mathbf{m}}G(\mathbf{m})$, where G denotes the free energy. The effective field is reduced to $\mathbf{\Gamma}_0 = (h_z + \beta m_z)\hat{\mathbf{z}}$, and therefore the components of Eq. (1) can be written as: $dm_z/d\tau = 0$, $dm_y/d\tau = (h_z + \beta m_z)m_x$ and $dm_x/d\tau = -(h_z + \beta m_z)m_y$. This set of equations has an exact family of homoclinic solutions:

$$m_{x,h}(\tau) = m_{x0}\cos(\Phi_0\tau) - m_{y0}\sin(\Phi_0\tau), \quad (3.a)$$

$$m_{y,h}(\tau) = m_{y0}\cos(\Phi_0\tau) + m_{x0}\sin(\Phi_0\tau), \quad (3.b)$$

$$m_{z,h}(\tau) = m_{z0}, \quad (3.c)$$

with period $T_{HO} = 2\pi/\Phi_0$ where $\Phi_0 = h_z + \beta m_{z0}$. The initial conditions have the modulus restriction $m_{x0}^2 + m_{y0}^2 + m_{z0}^2 = 1$. For a fixed free energy G, we obtain $m_{z0} = \beta^{-1}\left(-h_z \pm \sqrt{h_z^2 - 2\beta G}\right)$. Since m_{z0} must be real, the solutions are stable until $\beta_c = h_z^2/(2G)$. On the other hand, with dissipation and by the periodic injection of energy the magnetic particle is put into an out-of-equilibrium state.

III. Results

First, we characterize the dynamics of Eq. (1) by evaluating the Lyapunov exponents (LEs). This method consists of quantifying the divergence between two initially close trajectories of a vector field. [18]. In general, for an effective N-dimensional dynamical system described by a set of equations, $dX^i/d\tau = F^i(\mathbf{X}, \tau)$, the ith-Lyapunov exponent is given by $\lambda_i = \lim_{\tau\to\infty}\frac{1}{\tau}\ln\left(\|\delta X_\tau^i\|/\|\delta X_0^i\|\right)$, where $\|\delta X_\xi^i\|$ is the distance between the trajectories of the ith-component of the vector field at time ξ. They can be ordered in descending form, from the largest to the smallest: $\lambda_1 \geq \lambda_2 \geq .... \geq \lambda_N$. The first exponent is the largest Lyapunov exponent (LLE). Exploring the dependence of the LLE on the different parameters of the system, one can identify areas in parameter space, where the dynamics is chaotic (LLE positive), and those showing nonchaotic dynamics (LLE zero or negative). Since we are dealing with a two-frequency forced system, at least two of its Lyapunov exponents are always zero; hence the simplest attractor is a tori T^2 [16]. Another possibility is to have three Lyapunov exponents equal to zero and in this case the system shows a three-frequency QP behavior. We remark that a quasiperiodically driven system can exhibit other types of attractors, called strange nonchaotic attractors. They have a non-smooth topology but do not have a sensitive dependence on initial conditions (non-positive LLE) [17].
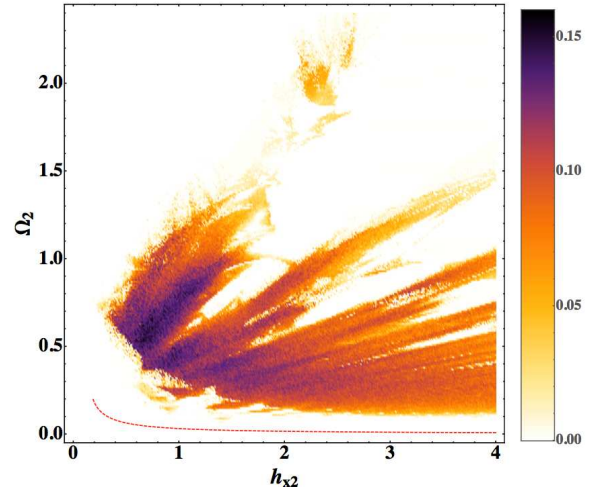

Fig 1: (Color online) The value of the largest positive Lyapunov exponent (LLE) is shown in a color-coded gauge as a function of the amplitude h_{x2} and frequency Ω_2 of the second driving field, with fixed $h_{x1} = 0.1$, $\Omega_1 = \pi/2$, $h_z = 0.1$, $\beta = 1$ and $\eta = 0.05$. The resolutions are $\Delta\Omega = \Delta h_{x2} = 10^{-2}$. The dashed (red) line depicts a solution of the zeros of the Melinkov function given by Eq. (5) in the text.

In contrast, there are other methods of quantifying the dynamical behavior of a system such as the Fourier spectrum, Poincaré sections, and correlation functions [1–8]. The classical one is the Fourier spectrum, which we denote by $S(f)$. Using this spectrum, one can define the spectral distribution function $N(\sigma)$ as the number of peaks of $|S(f)|$ with an amplitude greater than σ. This quantity obeys different scaling laws depending on the dynamical behavior. In particular, $N(\sigma) \propto \ln(1/\sigma)$ for a two-frequency quasiperiodic behavior, $N(\sigma) \propto (\ln(1/\sigma))^2$ for a three-frequency quasiperiodic behavior, and $N(\sigma) \propto \sigma^{-\alpha}$, with $1 < \alpha < 2$, for strange nonchaotic attractors [14, 17].

In order to integrate the equations of motion and avoid numerical artifacts, it is suitable to solve Eq. (1) in the Cartesian representation. In order to find the chaotic regimes, we have integrated Eq. (1) via a standard fourth order Runge-Kutta integration scheme with a fixed time step $d\tau = 0.01$ guaranteeing a precision of 10^{-8} for the magnetization field. The Lyapunov exponents are calculated using the technique exposed in Ref. [8], such that the error is of the order of 1%, which is sufficiently small for the purpose of the present analysis.
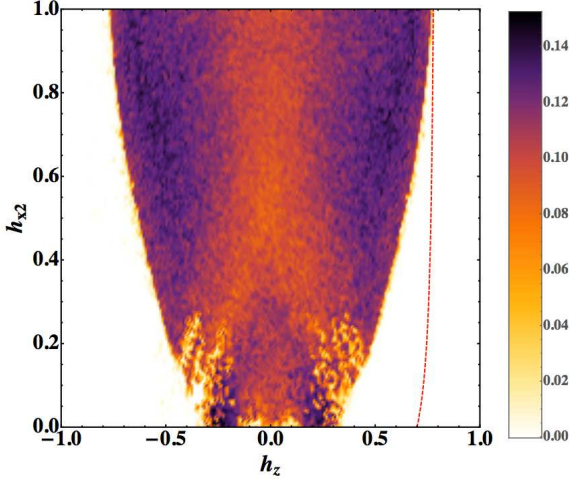

Fig 2: (Color online) The largest Lyapunov exponent (LLE) as a function of h_z and h_{x2}, with fixed $h_{x1} = 0.1$, $\Omega_1 = 1$, $\Omega_2 = \pi/4$, $\beta = 1$ and $\eta = 0.05$. The resolutions are $\Delta h_z = \Delta h_{x2} = 10^{-2}$. The dashed (red) line depicts a solution of the zeros of the Melinkov function given by Eq. (5) in the text.

Figure 1 shows the color-coded LLE as a function of amplitude h_{x2} and frequency Ω_2 of the second time dependent external field. There are no chaotic regimes for frequencies $\Omega_2 \gtrsim 2.4$, indicating that chaos occurs in the vicinity of the resonance condition. Obviously, chaos requires a sufficiently large value of the field amplitude, $h_{x2} \gtrsim 0.3$. Interestingly, inside the larger chaotic areas one can observe small chaos-free areas exhibiting rather complex boundary topologies between chaotic and regular regimes [18]. Finally, we observe that for small frequencies and field there are nonchaotic behavior. In fact, the dashed (red) line displays a branch of the zeros of the Melnikov function, which is given by Eq. (6) below. These zeros provide a threshold for regular behavior. Figure 2 shows the color-coded LLE as a function of both, the constant and the second oscillating field amplitude, h_z and h_{x2}, respectively. Here, the chaotic region occurs in a compact pattern of a rather characteristic shape. We found numerically that the chaotic region exists approximately inside the curve $h_{x2} \approx a |h_z|^p + b$, where $a = 2.38678$, $p = 3.59207$ and $b = -0.01$ for $h_{x2} \geq 0.05$. The dashed (red) line depicts the zeros of the Melnikov function. We observe that in both figures the theoretical calculations are fully compatible with the numerical simulations.

Figure 3 shows a 3D Poincaré section of $\mathbf{m}$ at time interval multiples of $2\pi/\Omega_1$ and the spectral distribution function,

$N(\sigma)$, as a function of σ for three different nonchaotic regimes (non-positive LLE) at three different values of h_{x1} with the other parameters fixed. From the Poincaré section we observe that, in the first two cases the curves are smooth and they are closed, while in the third frame the section is clearly non-smooth. In all cases we are performing a numerical fit. In the first case we found that $N(\sigma) = \mu \ln(1/\sigma)$ with, $\mu \approx 5.3$, in the second case $N(\sigma) = \mu \ln(1/\sigma)^2$ with $\mu \approx 1.05$, and finally in frame (c) the fit gives $N(\sigma) = \mu\sigma^{-\alpha}$, where $\mu \approx 0.46$ and $\alpha \approx 1.06$. The standard error of the fits are in the range $10^{-3} - 10^{-5}$. Hence, from these scaling laws we can conclude that for $h_{x1} = 0.4$ and $h_{x1} = 2.0$ the system exhibits a two-frequency and a three-frequency QP behavior, respectively; whereas for $h_{x1} = 27.67$ the system exhibits as a strange nonchaotic attractor.

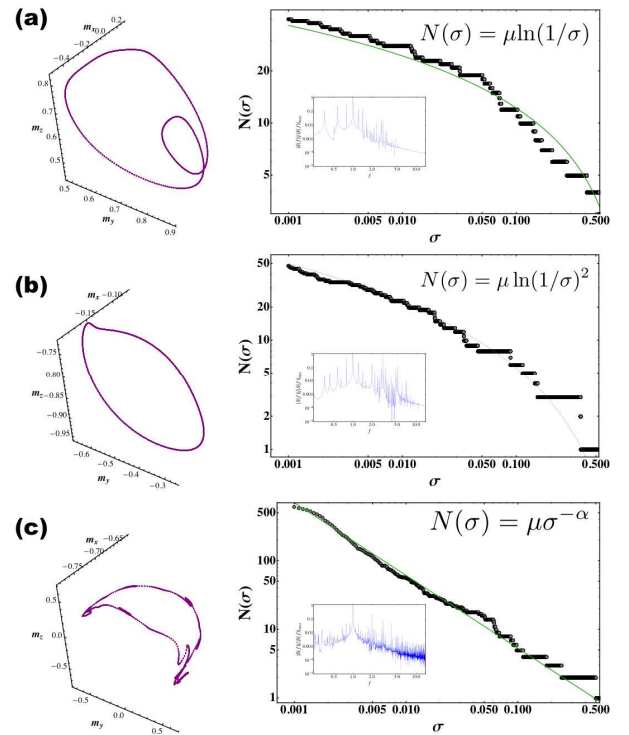
Fig 3: 3D Poincaré section of $\mathbf{m}$ at time interval multiples of $2\pi/\Omega_1$ and the spectral distribution function, $N(\sigma)$, as a function of σ for three different of h_{x1} at fixed $h_{x2} = 0.1$, $h_z = 0.1$, $\Omega_1 = 1$, $\Omega_2 = \pi/4$, $\beta = 1$, $\eta = 0.05$. The values of h_{x1} are $h_{x1} = 0.4$ (a), $h_{x1} = 2.0$ (b) and $h_{x1} = 27.67$ (c). The inset in $N(\sigma)$ displays the amplitude of the Fourier transform.

Since Eq. (1) is a nonlinear non-autonomous system, a complete theoretical description (with analytical solutions) is not possible. Nevertheless, there exists a criterion to calculate the bifurcation of HOs. This method uses the Melnikov function [2]. In order to perform this technique, let us introduce, instead of $\mathbf{m} = (\sin\theta\cos\phi, \sin\theta\sin\phi, \cos\theta)^T$, the canonical variables $\zeta = (\cos\theta, \phi)^T = (\zeta_1, \zeta_2)^T$ [2]. In these coordinates, Eq. (1) can be expressed as a two dimensional

vector equation $d\zeta/d\tau = \mathbf{f}_0(\zeta) + \mathbf{f}_1(\zeta,\varphi,\tau)$, where $\mathbf{f}_0$ accounts for the conservative term and $\mathbf{f}_1$ accounts for the time dependent magnetic field as well as the complete dissipative term. Here $\varphi = \{\eta, h_{x1}, \Omega_1, h_{x2}, \Omega_2\}$ is the set of control parameters. If we assume that the conservative system possesses a homoclinic solution $\zeta_{HO}(\tau)$, the Melnikov function is given by [2]

$$M(T_{HO}, \varphi) = -\int_0^{T_{HO}} d\tau \, \mathbf{f}_0(\zeta_{HO}(\tau)) \wedge \mathbf{f}_1(\zeta_{HO}(\tau), \varphi, \tau), \quad (4)$$

where $\mathbf{A} \wedge \mathbf{B} = A_1 B_2 \quad A_2 B_1$ and T_{HO} is the period of the HO. The marginal condition, when the homoclinic orbit becomes unstable, is given by $M(T_{HO}, \varphi) = 0$. This is a necessary condition for the occurrence of non-periodic behavior and gives a lower bound for the actual chaotic regime.

In our case $\mathbf{f}_0 = (0, h_z + \beta\zeta_1)$, hence we need of $\mathbf{f}_1$ only its first component, which is given by

$$f_{1,1} = \eta(1 - \zeta_1^2)(h_z + \beta\zeta_1) \pm h_x(\tau)\sqrt{1 - \zeta_1^2}(\sin\zeta_2 - \eta\zeta_1\cos\zeta_2).$$

In addition, the homoclinic orbit of the conservative system given by Eq. (3), which in (ζ_1, ζ_2)-representation can be written as $\zeta_{1,HO} = m_{z0}$ and $\zeta_{2,HO}(\tau) = \arctan(m_{yh}(\tau)/m_{xh}(\tau))$. Hence, after straightforward calculations, we find that Eq. (4) can be cast in the form

$$M = Q \pm \sum_{i=1}^{2} \frac{\Phi_0 h_{xi}}{\Delta\Omega_i}\left(\Lambda_i^{\left[\frac{3\pi}{2}\right]}\sin\frac{2\pi\Omega_i}{\Phi_0} + \Lambda_i^{[0]}\left(1 - \cos\frac{2\pi\Omega_i}{\Phi_0}\right)\right), \quad (5)$$

where, $Q = 2\pi\eta\Phi_0(1 - m_{z0}^2)$, $\Psi_{ab}^{\pm} = \pm m_{a0} + \eta m_{b0} m_{z0}$, $\Lambda_i^{[\xi]} = \Omega_i \Psi_{yx}^{-}\cos\xi + \Phi_0 \Psi_{xy}^{+}\sin\xi$ $\Delta\Omega_i = \Phi_0^2 - \Omega_i^2$. Figures 1 and 2 show part of some branches of the zeros of the Eq. (5) for the same parameters used in the numerical simulations and $m_{x0} = m_{y0} = 0.52$. One can observe that numerically found chaotic regions are on the *unstable* side of the Melnikov function, whose zeroes indeed act as a lower bound.

IV. SUMMARY

The dynamics of the magnetization of an anisotropic particle in the presence of both a constant and a two-frequency quasiperiodic time dependent external magnetic field has been studied using the Landau-Lifshitz-Gilbert equation. We have determined the parameter regions where a positive Lyapunov exponent exists and the theoretical bounds for the thresholds of the chaotic regime. Also, we found that the system exhibits strange non-chaotic attractors. Since in the present work the order of magnitude of the field and the frequencies is in the *kOe* and the *GHz* range, respectively, and since it is possible with the present technology to measure the ferromagnetic resonances in a wide range [10–13, 21], we suggest as experimental set-up nanodots with a size of $\sim 20\,nm$ (where the monodomain approximation is valid) under a quasi-periodic field, thereby observing the non-stationary behavior found numerically in the present work.

REFERENCES

[1] P.E. Wigen (Ed.), *Nonlinear Phenomena and Chaos in Magnetic Materials*, World Scientific, Singapore, 1994.

[2] I.D. Mayergoyz, G. Bertotti, and C. Serpico, *Nonlinear Magnetization Dynamics in Nanosystems*, Elsevier, North Holland, 2009; and references therein.

[3] D.V. Vagin and P. Polyakov, "Control of chaotic and deterministic magnetization dynamics regimes by means of sample shape varying", *J. App. Phys.*, vol. 105, 033914 (2009).

[4] D. Laroze and P. Vargas, "Dynamical behavior of two interacting magnetic nanoparticles", *Phys. B*, vol. 372, pp. 332-336 (2006); D. Laroze, P. Vargas, C. Cortes, and G. Gutierrez, "Dynamics of two interacting dipoles", *J. Magn. Magn. Mater.*, vol. 320, pp. 1440-1448 (2008).

[5] L.F. Alvarez, O. Pla, and O. Chubykalo, "Quasiperiodicity, bistability, and chaos in the Landau-Lifshitz equation", *Phys. Rev. B*, vol. 61, pp. 11613-11617 (2000).

[6] R.K. Smith, M. Grabowski, and R.E. Camley, "Period doubling toward chaos in a driven magnetic macrospin", *J. Magn. Magn. Mater.*, vol. 322, pp. 2127-2134 (2010).

[7] D. Laroze, O. J. Suarez, J. Bragard, H. Pleiner, "Characterization of the Chaotic Magnetic Particle Dynamics", *IEEE Trans. On Magnetics*, vol. 47, pp 3032-3039 (2011).

[8] J. Bragard, H. Pleiner, O. J. Suarez, P. Vargas, J. A. C. Gallas, and D. Laroze, "Chaotic dynamics of a magnetic nanoparticle", *Phys. Rev. E*, vol. 84, 037202 (2011).

[9] M.G. Clerc, S. Coulibaly, and D. Laroze, "Localized waves in a parametrically driven magnetic nanowire", *Europhys. Lett.*, vol. 97, 30006 (2012); D. Urzagasti, D. Laroze, M.G. Clerc, S. Coulibaly, and H. Pleiner, "Two-soliton precession state in a parametrically driven magnetic wire", *J. App. Phys.*, vol. 111, pp. 07D111 (2012).

[10] G. Gibson and C. Jeffries, "Observation of period doubling and chaos in spin-wave instabilities in yttrium iron garnet", *Phys. Rev. A*, vol. 29, pp. 811–818 (1984).

[11] F. M. de Aguiar, A. Azevedo and S. M. Rezende, "Characterization of strange attractors in spin-wave chaos", *Phys. Rev. B*, vol. 39, pp. 9448–9452 (1989)

[12] J. Becker, F. Rodelsperger, Th. Weyrauch, H. Benner, W. Just and A. Cenys, "Intermittency in spin-wave instabilities", *Phys. Rev. E*, vol. 59, pp. 1622-1632 (1999).

[13] J. Cai, Y. Kato, A. Ogawa, Y. Harada, M. Chiba and T. Hirata, "Chaotic dynamics during slow relaxation process in magnon systems", *J. Phys. Soc. Jap.*, vol. 71, pp. 3087-3091(2002).

[14] A. Bondeson, E. Ott, and T. M. Antonsen Jr., "Quasiperiodically Forced Damped Pendula and Schrödinger Equations with Quasiperiodic Potentials: Implications of Their Equivalence", *Phys. Rev. Lett.* vol. 55, pp. 2103–2106 (1985).

[15] T. Kapitaniak, and J. Wojewoda, *Attractors of Quasiperiodically Forced Systems*, World Scientific, Singapore, 1994; and references therein.

[16] M. Agrawal, A. Prasad, and Ram Ramaswamy, "Quasiperiodic forcing of coupled chaotic systems", *Phys. Rev. E* vol. 81, 026202 (2010).

[17] W. L. Ditto, M. L. Spano, H. T. Savage, S. N. Rauseo, J. Heagy, and E. Otth, "Experimental Observation of a Strange Nonchaotic Attractor", *Phys. Rev. Lett.*, vol. 65, pp. 533-536(1990); and references therein.

[18] J.A.C. Gallas, "The structure of infinite periodic and chaotic hub cascades in phase diagrams of simple autonomous flows", *Int. J. Bif. Chaos*, vol. 20, pp. 197-211 (2010); and references therein.

[19] X. Batlle and A. Labarta, "Finite-Size Effects In Fine Particles: Magnetic And Transport Properties", *J. Phys. D*, vol. 35, pp. R15-R42 (2002).

[20] P. Landeros, J. Escrig, and D. Altbir, D. Laroze, J. d'Albuquerque e Castro, P. Vargas, "Scaling relations for magnetic nanoparticles", *Phys. Rev. B*, vol. 65, 094435 (2005).

[21] F. G. Aliev, J. F. Sierra, A. A. Awad, G. N. Kakazei, D.S. Han, S. K. Kim, V. Metlushko, B. Ilic, and K. Y. Guslienko, "Spin waves in circular soft magnetic dots at the crossover between vortex and single domain state", *Phys. Rev. B*, vol. 79, 174433 (2009).